Surface Structure and Hydrogen Termination Effect of Cu/Si(111)

T.Koshikawa and T.Yasue

Fundamental Electronics Research Institute (FERI),
Osaka Electro-Communication University, Neyagawa, Osaka 572, Japan

(Received: Jan. 31, 1997 Accepted: Mar. 7, 1997)

Abstract

The Cu thin film processes on the clean Si(111)7×7 and the hydrogen terminated Si(111)δ7×7 surfaces have been in situ investigated by means of a high depth resolution medium energy ion scattering (MEIS), RHEED, AES and UHV-STM and ex situ observed with a field emission-secondary electron microscope (FE-SEM). The detailed film structure and the concentration profiles of Si in the Cu film deposited at RT were estimated by means of MEIS (depth resolution:0.1-0.4nm) and the computer simulation. The "5×5" incommensurate structure was also tried to be analyzed by means of the blocking profiles and the energy spectra which were obtained at ultra high depth resolution (~0.1nm) condition of MEIS and STM images.

On the other hand, on the hydrogen terminated Si(111) surfaces at RT, the growth processes are not different from those on the clean Si(111) surfaces. However, the formation processes of Cu on the hydrogen terminated Si(111) at HT (300-400°C) are quite different from those of the clean surfaces. This was clearly shown by the very different MEIS energy spectra, RHEED and FE-SEM images. The small size islands (~30nm) were observed on the clean surfaces, however, the triangular shaped islands whose size were ~1 μm were seen. The results predicts that the Cu atoms can easily migrate on the hydrogen terminated Si(111) surfaces and form the tall and big size islands.

1. Introduction

At high temperature (130-600°C), the quasi-5×5 ("5×5") layer by annealing or evaporation of about 1 monolayer(ML) Cu on Si(111) has a so-called incommensurate structure that has been discussed by a numerous number of reports, helium diffraction[1], LEED[2,3], angle-resolved AES[4], reflection electron microscopy (REM) [5], STM [6-11], scanning low energy electron microscopy[10], low energy electron microscopy (LEEM) [12], X-ray standing wave [13], angle resolved UPS and band calculation [14] etc. However, the models of the incommensurate structure so far reported have many varieties and have not yet been revealed. The present images of STM indicated that the domains of 5.5×5.5 periodicity were observed at the sample bias V_s>2V. The number density of Si atoms in the incommensurate layer was estimated by the paired dark and bright area of the "5×5" regions of STM images at less than 300°C [11]. Moreover the structure of Si at the bulk, which has no incommensurate layer, was investigated by the blocking profiles of medium energy ion scattering (MEIS) and also the Monte Carlo simulation of the ion trajectories. The double layer model is plausible [15]. The atomic layer position of Cu is also estimated by the ultra-high depth resolution (~0.1nm for Si bulk) measurement of MEIS.

The growth of Ag on the hydrogen terminated Si(111) surface has been widely investigated. The hydrogen termination of the Si(111) surface is made by the exposure of the atomic hydrogen to the clean surface or the chemical treatment in the pH-controlled HF solution. The Si(111) surface which is exposed to the atomic hydrogen at room temperature shows the δ7×7 structure [16] and the 1×1 structure reveals by the exposure at elevated temperature [17]. The HF treated surface also shows the 1×1 structure. Oura's group showed that the growth mode and the surface structure is altered on δ7×7 surface [18,19]. On the room temperature substrate, the orientation of the islands is well ordered. And the formation of the $\sqrt{3}\times\sqrt{3}$ structure is prevented and the islands whose structure is 1×1 grow at elevated temperature. The similar change of the growth processes is also reported for the HF treated 1×1 surface [20,21]. It is known that the Ag-Si system is a non-reactive one and the interdiffusion seldom occurs. On the contrary, the Cu-Si is one of the typical reactive system and the interdiffusion easily takes place. We will report and discuss the formation processes of Cu on the hydrogen terminated Si(111) surfaces by the in situ results of high depth resolution MEIS, RHEED and AES and ex situ surface morphological images a field emission scanning microscope (FE-SEM).

2. Experiments

For the analysis of "5×5" structure, the measurements with MEIS including AES and RHEED and STM were carried out in the different chambers. The images of the surface morphology was taken by the FE-SEM (Hitachi S-4100) ex situ.

Here we only describe the main points of the measurement conditions. For the measurements by MEIS whose schematic is shown in Fig.1, primary ion were He and the incident energy was 175keV. For the analysis of "5×5" structure, two primary angles were selected in order to check the blocking profiles carefully. The first angle was 35.3°, which is along the [110] axis, from the surface normal and the ion beam can "see" the first and second layers if the structure of Si has a same one of the bulk and there is no displacement. The second one was 60.5° along the [332] axis. The ion beam can "see" up to the fourth layer. For the measurements of the energy spectra at hydrogen terminated surfaces, the incident direction of the primary beam was along the [111] axis of the substrate (the incident angle of 70.5° from the surface normal). The scattered ions were detected using a toroidal electro-static analyzer over the scattering angle of 23° and the energy resolution ($\Delta E/E$) is about 4×10^{-3} [22]. The base pressure of the chamber is about 3×10^{-9} Pa. The working pressure during measurements was about 2×10^{-8} Pa. The typical depth resolution is 0.3-0.4 nm for the Cu substrate and 0.5-0.6 nm for the Si substrate which were estimated by the semi-empirical formula of Ziegler [23]. The measurements of ultra high depth resolution (~0.1 nm for Si) was performed by the grazing emission angles (2-5° from the surface).

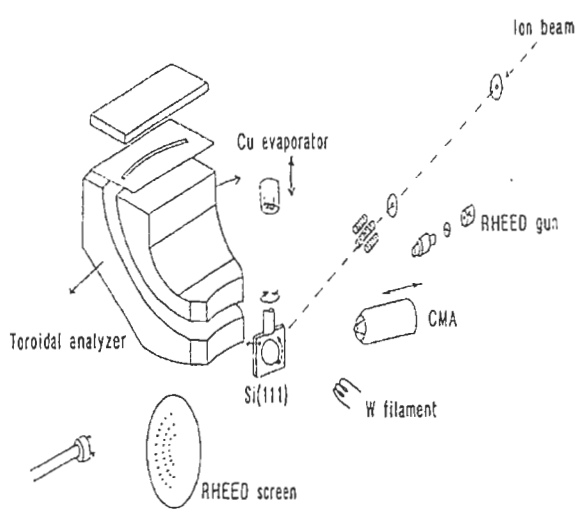

Fig.1 Schematic of the high depth resolution medium energy ion scattering

The STM images were taken with a field ion-STM (FI-STM) [23] with a constant current (50 pA) mode. The base pressure was 5.5×10^{-9} Pa and the pressure during measurements was better than 1.3×10^{-8} Pa.

The samples used in the measurements with MEIS and STM were the mirror polished B-doped p-type (1-100 Ω cm) and P-doped n-type Si(111) (1-10 Ω cm), respectively. The SEM images were observed with the samples which had been used for the measurements of MEIS. The samples were annealed at around 1200°C by direct resistive heating under a pressure below 6.7×10^{-8} Pa and then cooled down slowly to room temperature. Cu of 99.9999% was evaporated from Cu beads on hot tungsten wires. The deposition was around 1 ML/min. (1 ML=7.83×10^{14} atoms/cm^2) for MEIS and about 1/3 ML/min. for STM. The evaporation rate was monitored by the quartz oscillator.

The hydrogen termination was made by the exposure of the atomic hydrogen, which was generated by a hot W filament whose temperature was 1800°C, to the clean Si(111)7×7 surface at room temperature. With increasing the exposure of atomic hydrogen, the fractional order spots except for spots joining the integral order spots became weak. After the exposure was 1800L, the RHEED pattern showed the δ7×7 structure. Above 1800L, the RHEED pattern did not change so much. This experimental fact shows that the coverage of hydrogen might be nearly saturated. The saturated coverage was obtained by about 1.5 ML which was estimated by means of ERDA by Oura's group [25].

3. Results and Discussion

3.1 Structure analysis of "5×5" phase

The annealed surfaces (less than 300-600°C) from the early stage of the Cu deposition were observed by changing the sample bias. The reconstructed "5×5" regions after Cu evaporation at 400°C have random distinct protrusions and holes at a sample bias under 2V. These protrusions and holes have no clear relation with the "5×5" periodicity [7]. However, when the same part was displayed at a bias of over 2.5V, the "5×5" part shows clear regular domain protrusions whose periodicity is 5.5±0.2 times that of the silicon bulk [11], which is similar to the results of Mortensen [9]. However, images at a bias of 0.22V were

observed by him. We could observe regular domains at a low bias such as 0.22V after several times scanning of the surfaces. These bias dependence predicts that the tunneling images are strongly influenced by the surface electronic condition and the top of the tip condition. Why can we obtain the images of 5.5×5.5 time periodicity at a bias of over 2V? The spectra of an inverse photoemission of the "5×5" surface were published by Nicholls et al. [26]. The results indicate that a strong surface state at around 2.2eV above the Fermi level is present for a wide interval emission angles. This surface state might cause the clear 5.5 time periodicity of the STM images over V_s=2V.
Takayanagi et al. tried to proposed a model of the Si surface after estimation of the ratio of the "5×5" area on the upper and lower terraces [27]. They observed by REM that the "5×5" region grew up with nearly the same area on the upper and lower terraces at a single step. However, Bauer's group obtained different LEEM images in which there were some "5×5" regions on the center of the terraces [12]. We also observed that the "5×5" region at double step expanded to only upper or lower terraces These predict that the growth process of the "5×5" region is more complicated and might have temperature dependence. We tried to get the image at lower temperature (less than 300°C) in order to estimate the number density of Si atoms in the incommensurate layer. The paired "5×5" regions were seen on the same terrace. The ratio of S_D/S_B is 0.83 after averaging the data as shown in Fig.2. Here we assume that the structure at the top of the Si bulk has a double layer, which was predicted by the results of MEIS as shown in the later part of this section. We can estimate the number density N_i of Si atoms in the incommensurate layers as followers:

$$N_i=\{(N_{7\times7}-N_{double})S_B+N_{7\times7}S_D\} / (S_B+S_D)=0.99$$

where $N_{7\times7}$ is the number density of the 7×7 structure and N_{double} the density of the double layer. The value predicts that the incommensurate layer includes about 1 ML Si atoms. Here the conservation of Si atoms might be lost or added due to the migration from and to the steps. Such migration would influence the area of the bright and dark region and cause a large dispersion of the estimated value for the Si number density in the incommensurate layer [11]. However, the N_i estimated from the ratios

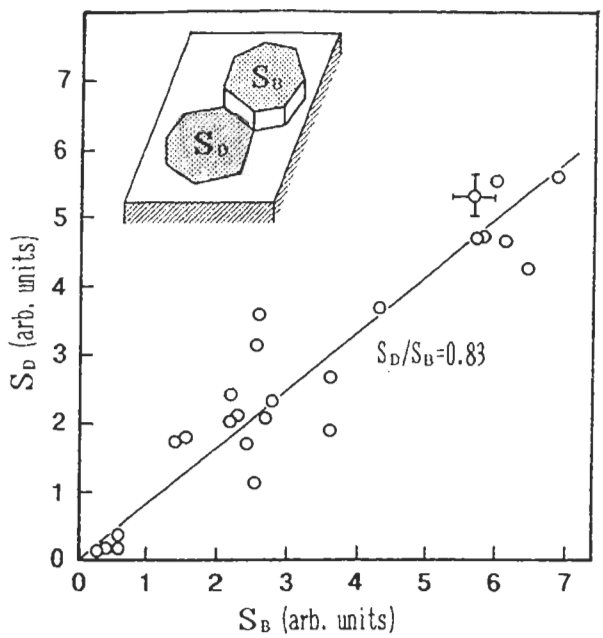

Fig.2 The relation between S_D (the dark area of "5×5" region) and S_B (the bright area). S_D/S_B is 0.83. The inset is the schematic of the STM image of the paired incommensurate regions.

which include most of the data falls in the range ±0.15 ML. It predicts that the assumption of the conservation of Si atoms might be reasonable.
The structure at the top of the Si bulk was investigated by the blocking profiles of MEIS of experiments and the simulation with the Monte Carlo method. Two models of the double layer and missing top layer are assumed. These two are the main models proposed so far. Each layer can be displaced in the simulation in order to fit the experiments [11,15]. Fig.3 shows the blocking profiles of the experiment (circle) and the simulation (solid lines: Fig3a for the double layer and Fig.3b for the missing top layer) for the primary angle of 35.3°. Assuming the displacement (0.01nm) of the first layer, the simulation profiles follow the experiments for the main dips of [$\bar{1}\bar{1}$3],[$\bar{1}\bar{1}$4] and [$\bar{1}\bar{1}$5], however, the medium dip at around 77° of the simulation based on the missing top layer model is not clearly seen in the experiments. This blocking dip is caused by scattering from the fourth and fifth layers, which is suggested by the simulation. For better reliability, the case of the primary angle 60.5° was also investigated by the experiment and the simulation. The dip at around 77° in the simulation for the missing top layer was emphasized due to the higher encounter probability of the primary ions to the fourth

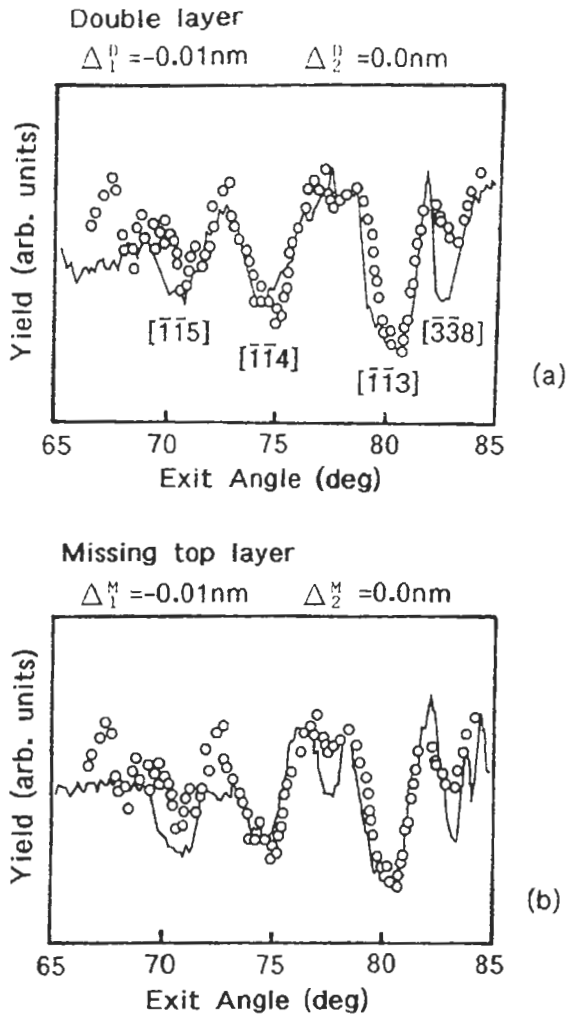

Fig.3 (a) Blocking profiles of the experimental (circles) and the simulation (solid line) results. Primary angle is 35.3° from the surface normal. The simulation profile is based on the double layer model and inward displacement of the first Si layer by 0.01nm. (b) The simulation profile (solid line) is based on the missing top layer model. The first layer of Si is also relaxed inward by 0.01nm.

layers. The dip cannot seen in the experiment. It predicts that the 7×7 structure of clean Si layer disappears and the double layer structure is constructed beneath the incommensurate layer. The detailed results for the position between Cu and Si layers in the incommensurate layer were estimated under the ultra- high depth resolution using the grazing emission angle (2-3° from the surface). The energy peak from the 1 ML Si in the incommensurate layer and each double layer of the Si bulk were separated. The Monte Carlo simulation which is based on the impact parameter dependent Oen and Robinson stopping power [28] and the uniform stopping power due to the surface and bulk plasmon [29]. Of course, there is some unknown ion scattering processes in the medium energy region, however, the tentative values of the distances between each layer were estimated after fitting the simulations to the experiments. There are two layers of Cu in the incommensurate layer. The distance is around 0.06nm. The distance between Si layer and the lower Cu layer is approximately 0.006nm. The position of the upper Si layer of the bulk is 0.18nm lower than that of the Si layer in the incommensurate layer.

3.2 Growth processes of Cu on the H-terminated Si(111)

The growth process of the Cu film at room temperature is at first discussed. Fig. 4 shows the backscattered energy spectra of MEIS for the clean Si(111)7×7 substrate (a) and for the hydrogen terminated Si(111) (b). The coverage of Cu was 13.1 ML. For the clean Si(111)7×7 substrate, the analysis of the energy spectrum has been as follows. The formed film thickness is not uniform and the average thickness is 2.0nm and the standard deviation of the thickness distribution is 0.23nm. Si layer of 0.07nm exists on the deposited film. The concentration of Si atoms at the interface of the film is 34% and has an exponential type decay whose decay length is 1.07nm [30]. Cu film can easily form the silicide which can be seen by the change (the split of Si splits into two peaks.) of AES spectra [31]. The details of the atomic and surface morphology were also observed by STM [32]. For the hydrogen terminated surfaces at room temperature, the same split was observed in AES spectra. Therefore the reaction of Cu with Si atoms is not suppressed by the hydrogen termination of the dangling bonds. The surface structure was also monitored by RHEED. The observed RHEED pattern showed that the 30° rotated film is formed on the hydrogen terminated substrate, which is the same with that on the clean Si(111)7×7 substrate. These experimental facts indicate that the effect of the hydrogen termination is not so serious at room temperature.

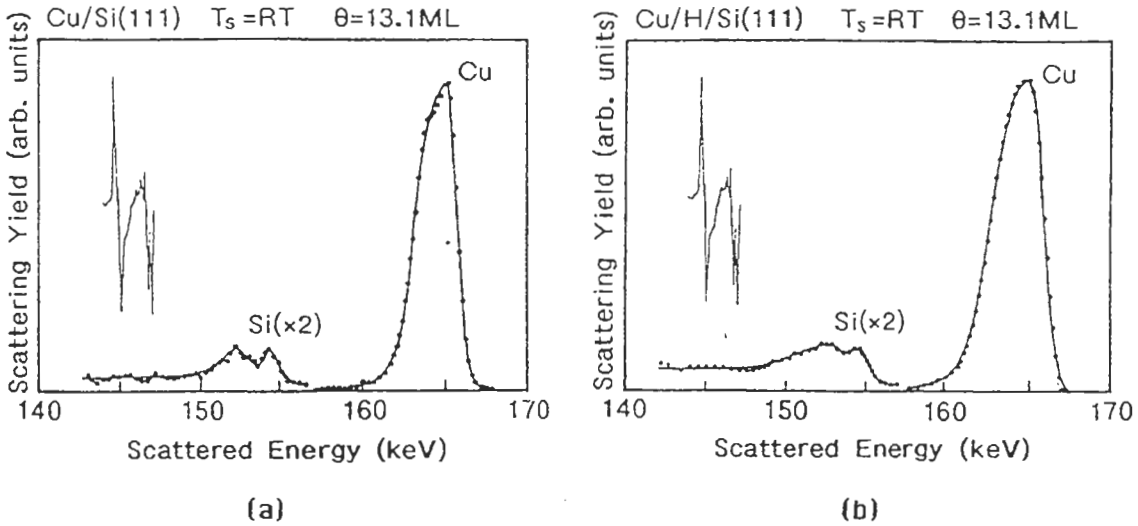

Fig.4 The backscattering energy spectra of MEIS for (a) Cu/Si(111) and (b) Cu/H/Si(111) surfaces. The coverage of Cu was 13.1 ML and the deposition was performed at room temperature.

At the elevated substrate temperature, it is observed that the growth processes are quite different between on the clean Si(111)7×7 and the hydrogen terminated Si(111). On the clean Si(111)7×7, the "5×5" structure is formed at 130-600°C. When the excessive Cu atoms (>1.3 ML) are deposited on the "5×5" structure, it is expected that the Cu atoms might diffuse into the bulk and/or might form the islands. Fig. 5(a) shows the energy spectra for Cu on the clean Si(111)7×7 surface. The substrate temperature (T_s) is 350°C and the coverage of Cu is 13.1ML. Dots are the experimental data and the solid line is drawn as a guide. In this spectrum, the sharp Cu and Si peaks are observed as well as the background. The Cu peak is induced by the 2D "5×5" layer. The background is due to the diffusion of Cu atoms into the bulk and/or the formation of the islands. By changing of T_s, the background level is changed. This is because the diffusion length and the height of the islands change with T_s. Also the background level changes by varying the coverage of Cu. For the hydrogen terminated Si(111) substrate at the elevated temperature, the spectral profile is quite different from that for the clean Si(111)7×7. Figs.5 (b)-(d) show the energy spectra of MEIS for the hydrogen terminated surfaces, where T_s is 280°C, 350°C and 390°C, respectively. The coverage of Cu is 13.1 ML for all cases. These spectra are composed by the broad Cu and sharp Si peak. With increasing T_s, the width of the Cu peak increases and the height of the Cu peak decreases. From these spectra it is concluded that the tall islands are formed on the hydrogen terminated surfaces. And the height of the islands increases with increasing T_s. Since the coverage of Cu is the same for all spectra, the coverage fraction of the whole surface by the islands becomes small with T_s. The area of the individual island might become small with increasing T_s. The Cu peaks show the tail. So the diffusion of Cu atoms into the substrate is also expected. In the energy spectra, the energy loss from the leading edge corresponds to the depth from the top of the islands. In Figs. 5(b)-(d) the maximum yield is seen at far from the edge. This indicates that the concentration of Cu atoms at the top of the islands is smaller than that in the islands. Therefore it is considered that the Si atoms segregate to the top of the islands and the mixed phase of Si and Cu is formed. The concentration of Si atoms, however, is not uniform. If the concentration was uniform, the Cu peaks should show a plateau near the leading edge. In the energy spectra the Cu yield gradually increases so that the concentration of Si atoms might be higher at the top of the islands and gradually decrease toward the inside of the islands. The other feature observed in the energy spectra is the presence of a structure at the leading edge of the Cu peak. At T_s=280°C, a knee is observed. There is a shoulder at T_s=350°C and the obvious peak is seen at T_s=390°C. It is plausible that the Cu peak consists of at least two contributions. One is the narrow peak at the leading edge and the other is the broad peak. The narrow Cu peak grows with increasing T_s. This facts indicate that the 2D layer co-exists with the islands on

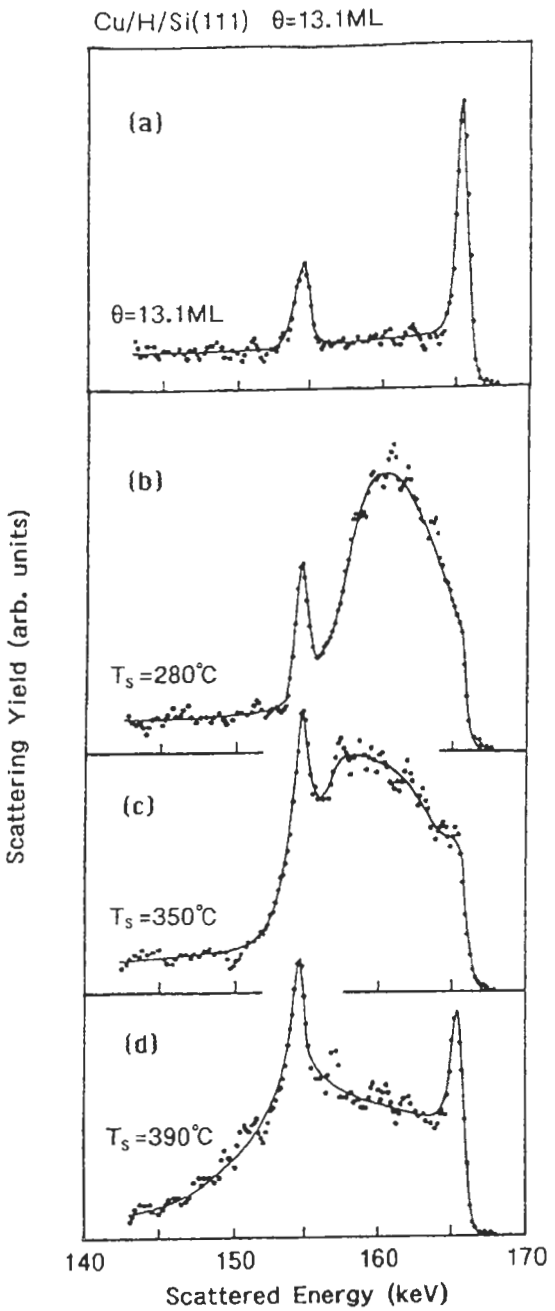

Fig.5 The backscattered energy spectra of MEIS. (a) The spectrum was measured for the Cu/Si(111)7×7 at T_s = 350°C with the coverage of 13.1 ML. (b)-(d) are the energy spectra for the Cu/H/Si(111). T_s is (b) 280°C, (c) 350°C and (d) 390°C. The coverage of Cu was 13.1 ML.

the hydrogen terminated surface. The area of the 2D layer increases with increasing T_s. At T_s=390°C, the weak "5×5" reflection is observed in the RHEED pattern. Then the 2D layer is the "5×5" structure. At the lower T_s, the area of 2D "5×5" region is so small that the "5×5" RHEED pattern is hardly recognized.

The presence of the islands was directly observed by means of SEM ex situ. Fig. 6(a) and (b) show the SEM image for the Cu/Si(111) and Cu/H/Si(111), which showed the "5×5" RHEED pattern, irregular shaped islands cover almost the whole surface. In the SEM image for the Cu/H/Si(111) surface, islands are also clearly recognized. However, the size and shape of islands is quite different from that for the Cu/Si(111) surface. The shape of the islands is mainly triangular and some islands are elongated along the side of triangule. It was difficult to recognize the 2D layer in the SEM image. Fig.6 (c) shows the size distribution of islands for the Cu/H/Si(111) surface. The average size is about 0.51μm^2 and the deviation is about 0.25μm^2. The length of the side of the triangle is 1μm. We also observed the SEM image for the coverage of 1.3 ML. The observed islands size is nearly the same with that observed in Fig.6. This indicates that the size of the islands changes by changing the coverage. The height of islands increases with the coverage, which will be shown below. In order to grow toward lateral direction, the breaking of the Si-H bond is required. The probability of the bond breaking might be determined by the temperature, so the size of the islands might depends on the substrate temperature. Comparing with the results for the Ag/H/Si(111) [33], the size of the islands is fairly large and the islands is tall in the case of the Cu/H/Si(111). The aspect ratio (height/lateral size of the islands) has been reported to be about 0.1 for the Ag/H/Si(111). Ohnishi et al. have been reported that the clustering of Ag is induced by the exposure of atomic hydrogen to the $\sqrt{3}\times\sqrt{3}$ structure [34]. They concluded that the migration of Ag atoms on the hydrogen terminated Si(111) surface is not so large and the clustering takes place on the $\sqrt{3}\times\sqrt{3}$ surface. On the hydrogen terminated Si(111) surface, it is considered that the migration of Cu atoms might be larger than that of Ag atoms. In the case of the Cu/H/Si(111), the density of the Cu dslands is small and the size of the individual islands becomes large because of the large migration of Cu atoms. Thus it is explained that the aspect ratio of the Ag islands on the hydrogen terminated substrate is larger than that of the Cu islands.

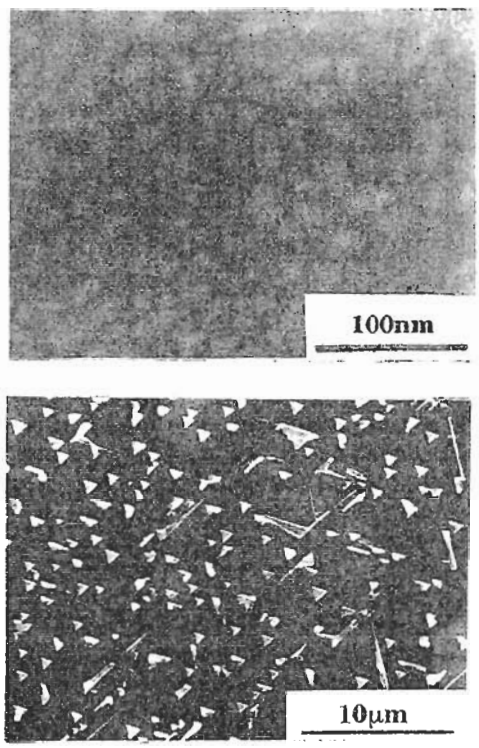

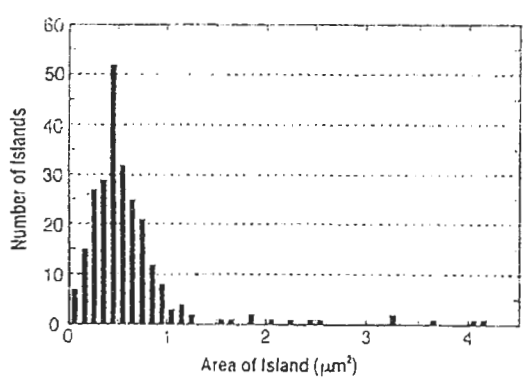

Fig.6 The SEM images observed for (a) Cu/Si(111) and (b) Cu/H/Si(111) surfaces which was prepared at T_s = 350°C. The coverage of Cu was 21.8 ML. (c) shows the size distribution of islands observed in Fig.6 (b).

Fig. 7 shows the energy spectra of MEIS for several Cu coverage. T_s is 350°C and the coverage of Cu is 1.3 ML, 5 ML and 13.1 ML in Figs.7 (a), (b) and (c), respectively. With increasing coverage, the width and height of the spectra becomes large. Therefore the height of the islands becomes large with the coverage. The contribution from the 2D layer, which is recognized at the leading edge of the Cu peak, grows with increasing coverage. This indicates that the area of the 2D "5×5" region also increases with the coverage. The RHEED pattern, however, shows that the δ7×7 structure remains. Therefore the hydrogen terminated Si(111) surface is still visible and the 2D layer does not cover the whole area. In comparison with the growth process at room temperature shown in Fig.4, it seems that Cu atoms can easily migrate on the hydrogen terminated surface at elevated temperature. The STM study for the hydrogen termination by Boland [35] indicates that the hydrogen covered Si(111) surface at room temperature is rough because of the existence of the Si hydride species. At elevated temperature of 370°C, the Si hydride species desorb and the 1×1 structure is observed [17]. Naitoh et al. showed that the Si hydride species is removed by Ag deposition at T_s=300°C [36]. In our case, the similar phenomena is plausible. At elevated temperature, Cu atoms might attack the surface Si hydride species and promote the desorption of hydrides. Then desorption of Si hydride species might be affected by the thermal activation and the attack of Cu atoms migrating

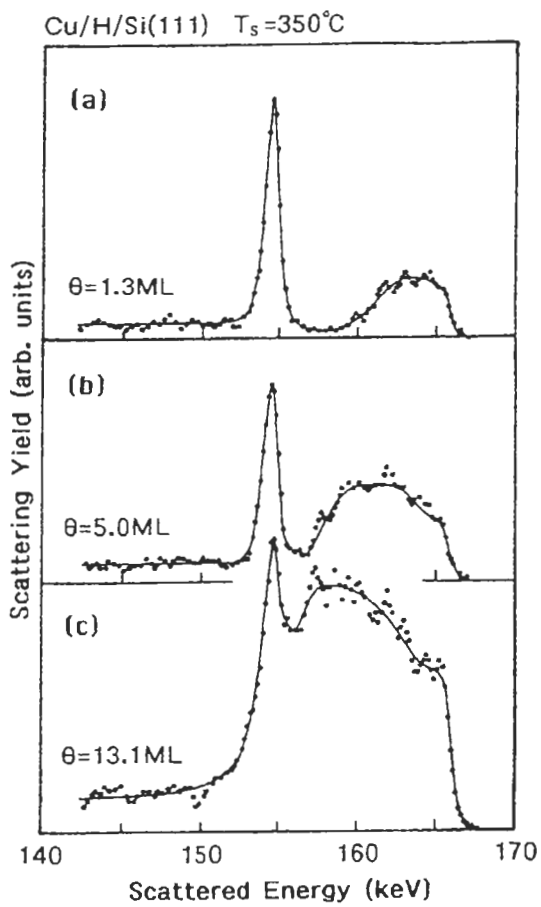

Fig.7 The backscattered energy spectra measured for the various coverage on the hydrogen terminated substrate. The coverage was (a) 1.3 ML, (b) 5 ML and (c) 13.1 ML. T_s = 350°C.

on the surface. The probability of the thermal activation depends in the substrate temperature. And the migration of Cu atoms on the surface might be controlled by the surface temperature, so it is considered that the probability of the desorption of hydrides also depends on the surface temperature. Murano and Ueda showed that the surface hydrogen amount decreases by annealing for the Ni/H/Si(111) with using ESD [37]. In their results the hydrogen signal starts to drop at about 250°C and gradually decreases after that. They concluded that there are two adsorption sites of hydrogen. It is considered that the first drop of the hydrogen signal is caused by the desorption of the higher order species. Therefore the desorption of the higher order hydrides might play an important role in the island formation process in the present case. Gradual desorption of the hydrogen from the 1×1 phase might induced the increase of the area of the 2D layer.

4. Conclusion

The structure of Cu on Si(111) at high temperature was proposed by the results of scanning tunneling microscope (STM) and high depth resolution medium energy ion scattering (MEIS). The STM images at high sample bias voltage show the very clear domains with 5.5 time periodicity that coincide to the "5×5" incommensurate structure. The atomic density (~1 ML) of Si in the incommensurate layer was estimated by the ratio of the area of the paired dark and bright "5×5" regions. In the structure of the Si bulk, the double layer structure is proposed and the top layer of the bulk Si displaces to the bulk by 0.01nm, which was obtained by the blocking profiles of the MEIS. The position of the Cu and the Si layer in the incommensurate layer was also discussed under the ultra-high depth resolution measurements.

The growth processes of Cu on the clean and the hydrogen terminated substrate are also observed, At room temperature, the hydrogen termination does not alter the growth process so much. However, when the substrate temperature is high enough to desorb the Si hydride species, the growth process is quite different from that for the clean Si(111) surface. The desorption of the higher order hydride formation of the islands takes place. The shape of the formed islands reflects the crystallographic orientation of the substrate. The size of the islands is influenced by the substrate temperature.

Acknowledgements

This work was partially supported by the Grand-in-Aid for Creative Basic Research (No. 08NP1201) and Grand-in-Aid for Scientific Research (08455026). We would like to thank M. Uno (Junior College, Osaka Electro-Communication University) for his kind help and advice in using the FE-SEM.

References

1. R.B.Doak and D.B.Nguyen, Phys. Rev. B 40 (1989) 1495.
2. E.Duagy, P.Mathiez, F.Salvan and J.M.Layet, Surf. Sci. 154 (1985) 267.
3. H.Kemann, F.Muller and H.Neddermeyer, Surf. Sci. 192 (1987) 11.
4. S.A.Chambers, S.B.Anderson and J.H.Weaver, Phys. Rev. B 32 (1985) 581.
5. K.Takayanagi, Y.Tanishiro, T.Inuzuka and K.Akiyama, Appl. Surf. Sci. 41/42 (1989) 337.
6. R.J.Wilson, S.Ching and F.Salvan, Phys. Rev. B 38 (1988) 12696.
7. St.Tosch and H.Neddermeyer, Surf. Sci. 211/212 (1989) 133.
8. J.E.Demuth, U.K.Korler, R.J.Hamers and P.Kaplan, Phys. Rev. Lett. 62 (1989) 641.
9. K.Mortensen, Phys. Rev. Lett. 66 (1991) 461.
10. T.Ichinokawa et al., Proc. of Symposium on Advanced Surface Analytical Technology, Ed. R.Shimizu (Jpn. Soc. Prom. Sci., 1997) in press.
11. T.Koshikawa, T.Yasue, H.Tanaka, I.Sumita and Y.Kido,Surf.Sci. 331-333 (1995) 506. T.Yasue, H.Tanaka, I.Sumita and T.Koshikawa, in preparation.
12. M.Munschau, E.Bauer, W.Telieps and W.Swiech, J. Appl. Phys. 65 (1989) 4747.
13. J.Zegenhagen, E.Fontes, F.Grey and J.R.Patel, Phys. Rev. B 46 (1992) 1860.
14. D.D.Chambliss and T.N.Rhodin, Phys. Rev. B 42 (1990) 1674.
15. T.Koshikawa, T.Yasue, H.Tanaka, I.Sumita and Y.Kido, Nucl. Instrum. Methods B 99 (1995) 495.
16. A.Ichimiya and S.Mizuno, Surf. Sci. 191 (1987) L765.
17. F.Owman and P.Martensson, Surf. Sci. 303 (1994) L367.
18. M.Naitoh, F.Shoji and K.Oura, Surf. Sci. 242 (1991) 152.
19. K.Sumitomo, T.Kobayashi, F.Shoji and K.Oura, Phys. Rev. Lett. 66 (1991) 1192.

20. R.Nail, C.Kota, B.U.M.Rao and G.W.Auner, J. Vac. Sci. Technol. A 12 (1994) 1832.
21. A.Nishiyama, G. ter Horst, P.M.Zagwijn, G.N. van der Hoven, J.W.M.Frenken, F.Garten, A.R. Schlatmann and J.Vrijmoeth, Surf. Sci. 350 (1996) 229.
22. T.Koshikawa, R.Kikuchi, K.Takagi, T.Uchiyama, Y.Mihara, Y.Agawa, S.Matsuura, E.Inuzuka and T.Suzuki, Nucl. Instrum. Methods B 33 (1988) 623.
23. J.F.Ziegler, He Stopping Powers and Ranges in All Elements (Pergamon, New York, 1997).
24. T.Sakurai, T.Hashizume, I.Kamiya, Y.Hasegawa, T.Ide, M.Miyao, A.Sasaki and S.Hyodo, J. Vac. Sci. Technol. A 7 (1989) 1684.
25. K.Oura, M.Naitoh, F.Shoji, J.Yamane, K.Umezawa and T.Hanawa, Nucl. Instrum Methods, B 45 (1990) 199.
26. J.Nicholls, F.Salvan and B.Reihl, Phys. Rev. B 34 (1986) 2945.
27. A.Shibata, Y.Kimura and K.Takayanagi, Surf. Sci. 275 (1992) L697.
28. O.S. Oen and M.T. Robinson, Nucl. Insrum. Methods 132 (1976) 647.
29. R. Kawai, N.Itoh and Y.Ohtsuki, Surf. Sci. 114 (1982) 137.
30. T.Yasue, C.Park. T.Koshikawa and Y.Kido, Appl. Surf. Sci. 70/71 (1993) 428.
31. G.Rossi and I.Lindau, Phys. Rev. B 28 (1983) 3597.
32. T.Yasue, T.Koshikawa, H.Tanaka and I.Sumita, Surf. Sci. 287/288 (1993) 1025.
33. M.Naitoh, F.Shoji and K.Oura, Jpn. J. Appl. Phys. 31 (1992) 4018.
34. H.Ohnishi, Y.Yamamoto, K.Oura, I.Katayama and Y.Ohba, J. Vac. Sci. Technol. A 13 (1995) 1438.
35. J.J.Boland, Surf. Sci. 244 (1991) 1.
36. M.Naitoh, A.Watanabe and S.Nishigaki, Surf. Sci. 357/358 (1996) 140.
37. K.Murano and K.Ueda, Surf. Sci. 357/358 (1996) 910.